Regenerative Therapy 7 (2017) 98–107

Contents lists available at ScienceDirect

Regenerative Therapy

journal homepage: http://www.elsevier.com/locate/reth

Original Article

The role of Tsukushi (TSK), a small leucine-rich repeat proteoglycan, in bone growth

Kosei Yano [a, b], Kaoru Washio [b], Yuka Tsumanuma [a], Masayuki Yamato [b, *], Kunimasa Ohta [c], Teruo Okano [b], Yuichi Izumi [a]

[a] Department of Periodontology, Graduate School of Medical and Dental Sciences, Tokyo Medical and Dental University (TMDU), 1-5-45 Yushima, Bunkyo-ku, Tokyo 113-8510, Japan
[b] Institute of Advanced Biomedical Engineering and Sciences, Tokyo Women's Medical University (TWIns), 8-1 Kawada-cho, Shinjuku, Tokyo 162-8666, Japan
[c] Department of Developmental Neurobiology, Graduate School of Life Sciences, Kumamoto University, 1-1-1 Honjo, Chuo-ku, Kumamoto 860-8556, Japan

ARTICLE INFO

Article history:
Received 21 June 2017
Received in revised form
7 August 2017
Accepted 14 August 2017

Keywords:
Tsukushi
SLRPs
Skeletal development
Endochondral ossification
Growth plate
Chondrocyte

ABSTRACT

Introduction: Endochondral ossification is one of a key process for bone maturation. Tsukushi (TSK) is a novel member of the secreted small leucine-rich repeat proteoglycan (SLRP) family. SLRPs localize to skeletal regions and play significant roles during whole phases of bone development. Although prior evidence suggests that TSK may be involved in the regulation of bone formation, its role in skeletal development has not yet been elucidated.

Methods: In the present study, we examined TSK's function during bone growth by comparing skeletal growth of TSK deficient (TSK−/−) mice and wild type (WT) mice. And an *in vitro* experiment using siRNA transfection of a chondrogenic cell line was performed.

Results: TSK−/− mice exhibited decreased weight and short stature at 3 weeks of age due to decreased longitudinal bone growth coupled with low bone mass. Furthermore, an *in vitro* experiment using siRNA transfection into a chondrogenic cell line revealed that decreased *TSK* expression induced down-regulation of key chondrogenic marker gene expression and up-regulation of mid-to-late chondrogenic markers gene expression.

Conclusions: Our results reveal that TSK regulates bone elongation and bone mass by modulating growth plate chondrocyte function and consequently, overall body size.

1. Introduction

Endochondral ossification is a key developmental process for most mineralized bone [1]. In this process, chondrocytes first differentiate from mesenchymal progenitors. Growth plate chondrocytes proliferate and undergo multiple maturation phases to differentiate into hypertrophic chondrocytes after lineage commitment [2,3]. The differentiated chondrocytes terminally turn into mineralized cartilage, which is replaced by bone. Multiple signaling pathways are associated with these processes [4]. However, the precise underlying mechanisms of these steps are not well understood. Understanding the mechanism of cartilage and bone growth is significant for regenerative medicine for skeletal diseases.

Tsukushi (TSK) was originally identified by signal sequence trap screening using a chick lens library [5]. TSK is a unique member of the secreted small leucine-rich repeat proteoglycan (SLRP) family [6]. SLRP family members can bind to the other components of extracellular matrix (ECM), such as collagen, growth factors in ECM, such as bone morphogenetic protein (BMP), transforming growth factor (TGF), and fibroblast growth factor (FGF), leading to the modulation of cellular functions [6,7]. SLRPs localize to skeletal

Abbreviations: TSK, Tsukushi; SLRP, small leucine-rich repeat proteoglycan; ECM, extracellular matrix; BMP, bone morphogenetic protein; TGF, transforming growth factor; FGF, fibroblast growth factor; EDTA, ethylenediaminetetraacetic Acid; TRAP, tartrate-resistant acid phosphatase; WT, wild type; FBS, fetal bovine serum; ITS, insulin-transferrin-selenium supplements; β-gal, β-Galactosidase.

* Corresponding author. Institute of Advanced Biomedical Engineering and Science, Tokyo Women's Medical University, 8-1 Kawada-cho, Shinjuku-ku, Tokyo 162-8666, Japan. Fax: +81 3 3359 6046.
E-mail address: yamato.masayuki@twmu.ac.jp (M. Yamato).

Peer review under responsibility of the Japanese Society for Regenerative Medicine.

http://dx.doi.org/10.1016/j.reth.2017.08.001

regions and have significant roles during whole phases of bone development [8]. SLRP depletion is deeply correlated with phenotypes or degenerative diseases such as short stature [9], osteoporosis, and ectopic bone formation [8].

Structurally, TSK is categorized as a class IV SLRP [6], although it shares functional properties with class I SLRPs [5,10], including biglycan, decorin, and asporin. Biglycan-deficient mice exhibit decreased body and bone length, mineral density, and bone mass [11–13]. In addition, biglycan and decorin are known to modulate skeletal growth and bone formation through interacting with TGF-β [8]. Asporin also interacts with TGF-β and reduces its signal effect by inhibiting it from binding to its receptor [14].

TSK inhibits signal molecules such as BMP, TGF-β, Wnt, and FGF [5,15–17]. TSK acts as an important coordinator of numerous pathways outside the cell through regulating the extracellular signaling network [18]. TSK deletion in mice causes defects in anterior commissure tract formation in the brain [19] and cell differentiation delay in the hair cycle by regulating TGF-β1 [17]; however, no skeletal phenotype has been reported. Paracrine factors including FGFs [20–23], BMPs [24–26], and Wnts [27,28] are necessary for normal growth plate function or skeletal development.

Although prior evidence suggests that TSK has a potential of function in the regulation of bone formation, its role in skeletal development has not yet been elucidated. In the present study, we utilized a TSK deficient (TSK−/−) mouse model to compare skeletal growth of TSK deficient (TSK−/−) mice and wild type (WT) mice. Additionally, an *in vitro* experiment using siRNA transfection of a chondrogenic-mesenchymal cell line was performed to examine the further functions of TSK during bone and cartilage growth.

2. Methods

2.1. Ethics statement

All experiments on mice were performed according to protocols approved by the guidelines of the Animal Welfare Committee of Tokyo Women's Medical University.

2.2. Mice

The TSK−/− mice were provided by Kumamoto University, which were generated by replacing the TSK coding exon with a LacZ/Neo cassette [19]. Mice were backcrossed more than 6 times to the C57BL/6J strain and can be considered to derive from an almost uniform genetic background. TSK−/− mice were viable and fertile, and no abnormal behavior was observed. Mice were housed under conventional conditions on a 12-h light/dark cycle at the Institute of Laboratory Animals, Tokyo Women's Medical University. Mice were housed in individually ventilated cages in a temperature-controlled environment and were provided standard rodent chow. Mice were euthanized with cervical dislocation after inhalation of isoflurane. Three-week-old mice were used as juveniles and 20-week-old mice as adults.

For genotyping, DNA was extracted from the lysates from tail biopsies and was applied to PCR kit (Finnzymes; Thermo Fisher Scientific, USA) for the determination of the presence of TSK with the appropriate primers as follows: 5′-cccagcagtagcaacaacaa-3′ (TSK-S), 5′-gagcttgtaagtcccttgga-3′ (TSK-AS), and 5′-gatccccatcaagattatcg-3′ (LacZ).

2.3. Measurement of body length, weight, and food intake

WT and TSK−/− mice were analyzed for stature and weight. WT and TSK−/− mice were measured from the top of the head to the base of the tail ($n = 4$). WT and TSK−/− mice were weighed weekly from 3 weeks to 10 weeks of age ($n = 10$). At 3 weeks of age, mice were individually housed to assess food intake. Water and food were provided *ad libitum*. Food intake was assessed as the difference in food weight before and after the 24-h period of individual housing ($n = 4$).

2.4. Radiologic analysis

X-ray pictures of whole mouse skeletons were obtained by X-ray irradiation at 30 kV and 5 mA for 2 s using a Softex system (Softex Co, Kanagawa, Japan). Extracted femurs were fixed with 4% paraformaldehyde for 24 h and were stored at 4 °C. Femurs were extracted from 3- and 20-week-old male WT and TSK−/− mice and subjected to 3D-μCT (Rigaku, Tokyo, Japan). Femur lengths were measured with 3D-μCT ($n = 4$). The obtained X-ray images were quantified with bone morphometry software (TRI/3D-BON; Ratoc, Tokyo, Japan). A cylinder with a length of 1.0 mm located 0.4 mm proximal to the distal growth plate was delineated as a region of interest containing the secondary trabecular bone. Trabecular bone volume per tissue volume, trabecular thickness, trabecular number, trabecular separation, and cortical thickness were analysed with CT software (TRI/3D-BON; Ratoc, Tokyo, Japan) ($n = 4$). Cortical thickness was measured at the middle of the femur shaft and calculated for each section by using the mean of 8 randomly placed lines ($n = 4$).

2.5. Bone marrow cell culture

Bone marrow cells were harvested from femur of 20-week-old WT and TSK−/− mice. For osteoblast differentiation, bone marrow cells were seeded in 96-well plate at a cell density of 2×10^5 cells/ml and cultured in α-MEM (Sigma–Aldrich, St Louis, MO, USA) medium containing 10% fetal bovine serum (FBS, Japan Bioserum, Hiroshima, Japan) and osteoinductive supplements (82 μg/ml ascorbic acid, 10 mM beta-glycerophosphate, and 10 nM dexamethasone) at 37 °C for 14 days. And then, mineralized nodules were stained by alizarin red S and stained area were measured and analyzed with Image J software (NIH). For osteoclast differentiation, bone marrow cells were seeded in 96-well plate at a cell density of 0.5×10^5 cells/ml and cultured with osteoclast-inductive medium (Osteoclast Culture Kit, Cosmo Bio, Tokyo, Japan) at 37 °C for 7 days. And then, cells were stained by tartrate-resistant acid phosphatase staining using TRAP staining kit (Cosmo Bio, Tokyo, Japan) and the number of osteoclasts was counted.

2.6. Histology

For alcian blue/alizarin red skeletal staining, new born littermates (postnatal day 2) were fixed with 95% ethanol for 4 days and double-stained with alcian blue and alizarin red to evaluate skeletogenesis as described previously [29].

For β-galactosidase (β-gal) staining, unfixed extracted femurs were immediately embedded in SCEM compound (Leica Micro System, Tokyo, Japan), and frozen blocks were prepared into 10-μm frozen sections. LacZ staining was performed using a β-gal staining set (Roche, Basel, Switzerland) following the manufacturer's recommendations to assess sites of expression of TSK in the femur. Slides were dried for 30 min at room temperature and stained for 6 h at 37 °C in a solution containing 400 μg/ml X-gal. After washing in H_2O for 1 min at room temperature, slides were counterstained with 1% nuclear fast red (Wako, Tokyo, Japan) solution for 3 min and washed.

To prepare decalcified paraffin sections, samples were demineralized in 4% Ethylenediaminetetraacetic Acid (EDTA). After

paraffin embedding, sections were subjected to haematoxylin and eosin staining or toluidine blue staining. Mean height of resting, proliferating and hypertrophic zones of growth plates, which were distinguished by cellular morphology from histological observation, were calculated for each section by using the mean of 10 randomly placed lines ($n = 3$).

2.7. ATDC5 cell culture

A mouse embryonal carcinoma-derived chondrogenic cell line (ATDC5) was purchased from the Riken BioResource Center. ATDC5 cells were cultured in Dulbecco's modified Eagle's medium and Ham's F12 medium (DMEM/F12; Sigma–Aldrich, St Louis, MO, USA) supplemented with 5% fetal bovine serum (FBS, Japan Bioserum, Hiroshima, Japan).

To induce chondrogenic differentiation of ATDC5 cells, medium was added with Insulin-Transferrin-Selenium Supplements [ITS, 10 μg/ml bovine insulin (Sigma–Aldrich, St Louis, MO, USA), 10 μg/ml human transferrin (Sigma–Aldrich), and 3×10^{-8} M sodium selenite (Sigma–Aldrich)]. Under differentiation conditions, the medium was changed every other day. To assess TSK function, siRNA designed to target the *TSK* gene (MSS216917, Thermo Fisher) was transfected into ATDC5 cells. Stealth RNAi™ siRNA Negative Control (Med GC, 12935300, Thermo Fisher) was used as a control.

For the differentiation assay, ATDC5 cells were cultured in micromass cultures as described previously [30]. Briefly, ATDC5 cells were suspended in DMEM/F-12 (1:1) medium containing 5% FBS at a cell density of 1×10^7 cells/ml. Then, 10-μl droplets added to the wells of a 24-well plate and cultured at 37 °C for 1 h. To simulate high-density chondrogenic condensation, 1 ml of culture medium supplemented with ITS was added to each well, and wells were cultured for 7 d. The medium was replaced every other day. Then, cells were fixed with 0.1% glutaraldehyde at 20 °C for 20 min, washed with phosphate-buffered saline (PBS), and stained with 0.5% alcian blue (Wako, Tokyo, Japan) for 6 h before being washed with 0.1 M hydrochloric acid. Stained nodule areas were measured and analyzed with Image J software (NIH) ($n = 6$).

To determine the effect of TSK depletion on chondrogenic differentiation markers, *TSK* siRNA was added to the medium 1 day after ATDC5 cells were seeded in DMEM/F-12 (1:1) medium containing 5% FBS at a cell density of 0.5×10^5 cells/35-mm well. ITS was added 3 days after siRNA was transfected into ATDC5 cells. The induction medium was replaced every other day, and ATDC5 cells were harvested at days 3, and 7 of differentiation culture. In each time point, total RNA was extracted ($n = 3$).

2.8. Real-time RT-PCR

For gene expression analysis from mouse tissue that were captured by laser microdissection (LMD), unfixed mouse femurs were harvested and were immediately embedded in SCEM compound (Leica Micro System, Tokyo, Japan). Frozen sections were prepared at a thickness of 6 μm with an LMD Cryofilm (Leica Micro System) using a CM3050S cryomicrotome (Leica, Nussloch, Germany), according to the method described by Kawamoto [31]. Sections were dried at room temperature for 1 h and briefly fixed with 100% ethanol. Each growth plate zone was individually captured and microdissected from cryosections using PALM MicroBeam (Carl Zeiss MicroImaging, Jena, Germany) and was placed on the dip in the lid of a 0.5-ml tube with TRIzol (Thermo Fisher) ($n = 4$). RNeasy Micro Kits (Qiagen, Hilden, Germany) were used for extracting RNA. Total RNA was digested with DNase to eliminate any contaminating genomic DNA. For RT-PCR analyses, 300 ng of total RNA was reverse-transcribed into first-strand cDNA using a Superscript VILO cDNA Synthesis Kit (Invitrogen, Thermo Fisher Scientific, Waltham, MA, USA) and primers. RNeasy Mini Kits (Qiagen) were used for extracting RNA from ATDC5 cells, and the amount of total RNA used in amplification was 500 ng. PCR amplification was performed in a reaction volume of 20 μl containing 1 μl of cDNA and 10 μl of qPCR Master Mix (Applied Biosystems, Foster City, CA, USA). mRNA expression levels were quantitatively analysed by real-time RT-PCR using sequence-specific primers and probes (Applied Biosystems, Foster City, CA, USA) for *TSK* (5′-CATTCGGCCTCTTTG-3′), *Sox9* (Mm00448840_m1), *Runx2* (Mm00501584_m1), *Col2a1* (Mm01309565_m1), *Col10a1* (Mm00487041_m1), *and Mmp13* (Mm00439491_m1), with using the StepOnePlus RT-PCR system (Applied Biosystems). B2-microglobulin (*B2M*), an appropriate reference gene for RT-PCR [32], was used as the internal control gene, and fold changes were calculated using the values obtained by the ΔΔCT method at each time point.

2.9. Statistical analysis

An unpaired *t*-test was performed to compare WT and TSK−/− mouse samples using Excel (Microsoft). A p-value < 0.05 indicated a significant difference.

3. Results

3.1. TSK−/− mice exhibited reduced body length, body weight, and shorter skeletons

TSK−/− mice exhibited no obvious viability or fertility problems and abnormal behaviors. At 3 weeks of age, the body length from the top of the head to the base of the tail was significantly reduced in TSK−/− mice (Fig. 1A and B). Body weight was measured weekly in wild-type (WT) control mice and TSK−/− mice during postnatal mouse development from 3 weeks to 10 weeks. TSK−/− mice weighed significantly less than their WT littermates in each time point (Fig. 1C). In addition, TSK−/− mice displayed skeletal size reduction and no obvious skeletal degenerative diseases were observed as shown in Fig. 1D. The femur lengths of WT and TSK−/− mice were measured at 3 and 20 weeks of age with three-dimensional micro-computed tomography (3D-μCT). TSK−/− mice displayed a significant reduction in femur length revealing a delay in longitudinal bone growth when compared with that of WT littermates (Fig. 1E). Additionally, in order to further examine skeletal features of TSK−/− mice, double skeletal staining was performed. The double-stained skeletal specimen exhibited that TSK−/− mice showed smaller skeletons with the size reduction of cartilage area (Fig. 1F). Therefore, TSK−/− mice exhibited phenotypic features such as decreased weight as well as short stature due to decreased longitudinal growth of long bones.

Nutritional intake can affect longitudinal bone growth and consequently body size, and therefore food intake was measured. Results showed no significant difference in food intake between 3-week-old WT and TSK−/− mice (Fig. 1G). The reductions in the body weight and size of TSK−/− mice are therefore unrelated to food intake.

3.2. Lower femur bone mass in TSK−/− mice

In order to compare microstructure and composition of bone in 3- and 20-week-old WT and TSK−/− mice, bone morphometric analyses of mouse femurs were conducted using 3D-μCT. The trabecular regions and cortical regions were separately analyzed as shown in Fig. 2A. Reduction of bone mass in 3-week-old TSK−/− mice was observed in the trabecular bone, showing an approximately 70% reduction in the bone volume/tissue volume ratio (Fig. 2B, C, E). Twenty-week-old TSK−/− mice also exhibited

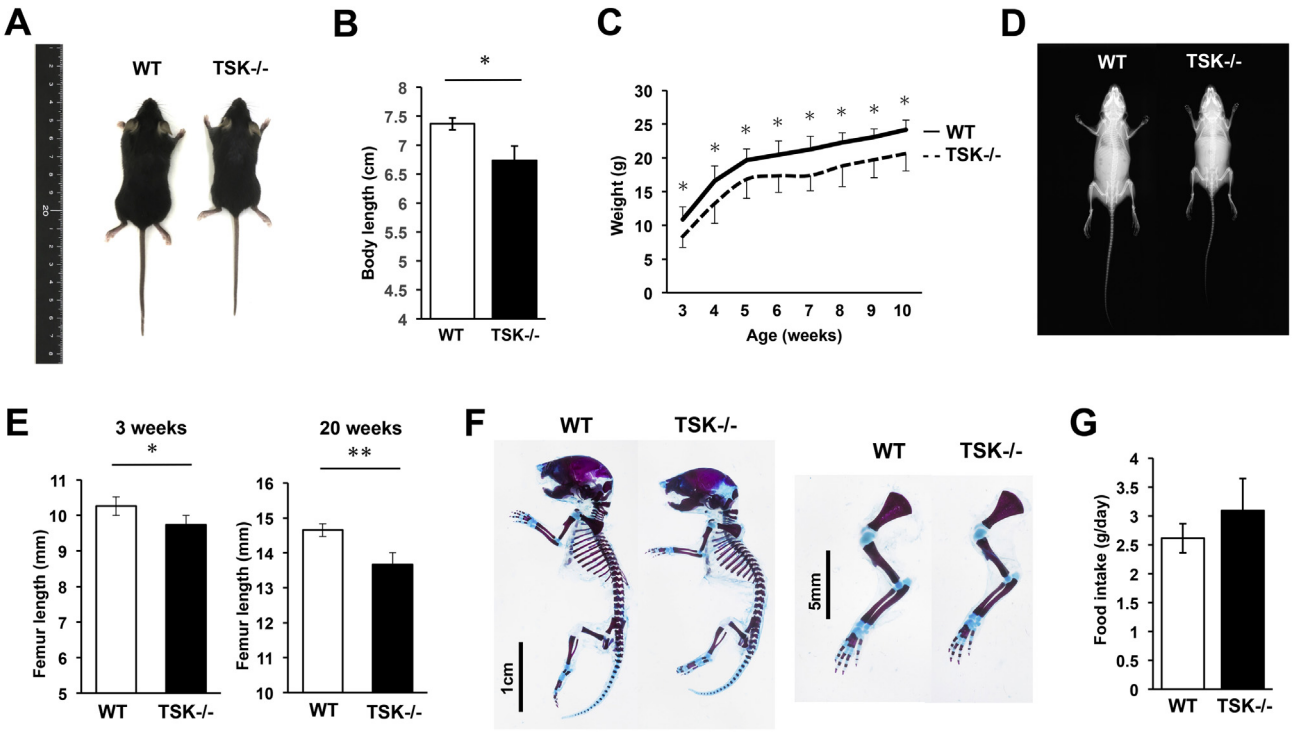

Fig. 1. TSK−/− mice exhibited reduced body weight and shorter skeletons. (A) Representative whole-body macrograph images of WT and TSK−/− mice at 3 weeks of age showing reduced body size in TSK−/− mice compared with that of WT littermates. (B) Body length measurements recorded at 3 weeks of age from the top of the head to the base of the tail. TSK−/− mice showed a significant reduction in size ($^*p < 0.05$ vs. WT littermates, $n = 4$). (C) Body weight measurements recorded during postnatal mouse development from 3 weeks to 10 weeks. TSK−/− mice weighed significantly less than their WT littermates at each age ($^*p < 0.05$ vs. WT littermates, $n = 10$). (D) Representative whole-body X-ray images showing reduced skeletal size in TSK−/− mice at 3 weeks of age compared with that of WT littermates. (E) Femur lengths of TSK−/− and WT mice, displaying a significant reduction in femur length in TSK−/− mice both at 3 and 20 weeks of age ($^*p < 0.05$, $^{**}p < 0.01$ vs. WT littermates, $n = 4$). (F) Representative images of skeletal stains of P2 new born littermates with alcian blue and alizarin red staining. TSK−/− mice showed the size reduction of cartilage area. (G) Food intake of 3-week-old WT and TSK−/− mice over 24 h. There was no significant difference between WT littermates and TSK−/− mice ($n = 4$, NS).

reduction of bone mass the same as showed in juvenile TSK−/− mice (Fig. 2F). Additionally, the bone microstructure in TSK−/− mice was deteriorated, as evidenced by significant decreases in trabecular number and trabecular thickness (Fig. 2E and F). These skeletal phenotypic features were observed in juvenile mice and lasted up to adult mice.

For cortical bone examination, a region of interest was located in the mid-shaft area of the bone, and the cortical thickness was measured within this area. Cortical thickness was not significantly different between juvenile WT and TSK−/− mice. However, cortical thickness was significantly reduced in adult TSK−/− mice compared with that of WT littermates (Fig. 2D, G).

For elucidating the mechanism of decrease in bone mass in TSK−/− mice, we considered contribution of TSK's defects in osteoblasts and osteoclasts. Bone marrow cells were harvested from femur of 20-week-old WT and TSK−/− mice and cultured with osteoinductive medium containing ascorbic acid, beta-glycerophosphate, and dexamethasone. And then, mineralized nodules were stained by alizarin red S and stained area were compared. There was no significant difference in nodule formation activity between WT and TSK−/− osteoblasts (Fig. 2H). So we assume that decrease in bone mass is not due to osteoblasts function in TSK−/− mice. On the other hand, when bone marrow cells were harvested from femur of WT and TSK−/− mice and cultured with osteoclast-inductive medium, and then, stained by tartrate-resistant acid phosphatase (TRAP) staining and the number of osteoclasts was counted. The number of TRAP-positive cells was significantly increased in TSK−/− mice (Fig. 2I). This result indicates that TSK possibly effects bone volume by regulating osteoclast differentiation in bone marrow in adult stage. However, the result of osteoclast formation needs to be considered the effect of age-related change, such as osteoporosis. In this study, we focused on TSK's role on bone growth because phenotypic features of TSK−/− mice are confirmed from their juvenile stage.

3.3. *Shortened and morphologically abnormal growth plates in TSK−/− mutant femurs*

Endochondral ossification is the essential mechanism for longitudinal development of long bones. To investigate whether TSK is involved in endochondral ossification and consequently resulting long bone growth and development, femurs of 3-week-old TSK−/− mice were frozen-sectioned, and β-gal staining was conducted to visualize expression pattern of TSK. Expression can be monitored by X-gal staining because a gene encoding β-galactosidase is replaced with TSK gene locus. TSK was widely expressed in almost all bone regions in the femurs of juvenile mice (Fig. 3A). TSK expression was observed in chondrocytes in the growth plate and in cells around the trabecular bone and cortical bone (Fig. 3A). We also performed whole-mount β-gal staining using TSK−/− mice at P0 and we have confirmed that cells on humerus and costal cartilage were stained (data not shown). No endogenous β-gal activity was observed in the femurs of WT mice in our experiments (Fig. 3A).

In addition, femur growth plates of 3-week-old TSK−/− mice were observed histologically. Haematoxylin and eosin (H-E) staining showed that the columnar array of chondrocytes in femur growth plates was disturbed and tissue structure was deteriorated in TSK−/− mice (Fig. 3B). And thickness of each growth plate cartilage zone was measured to confirm the effect of TSK for chondrogenesis. As shown in Fig. 3C, growth plate thickness was reduced

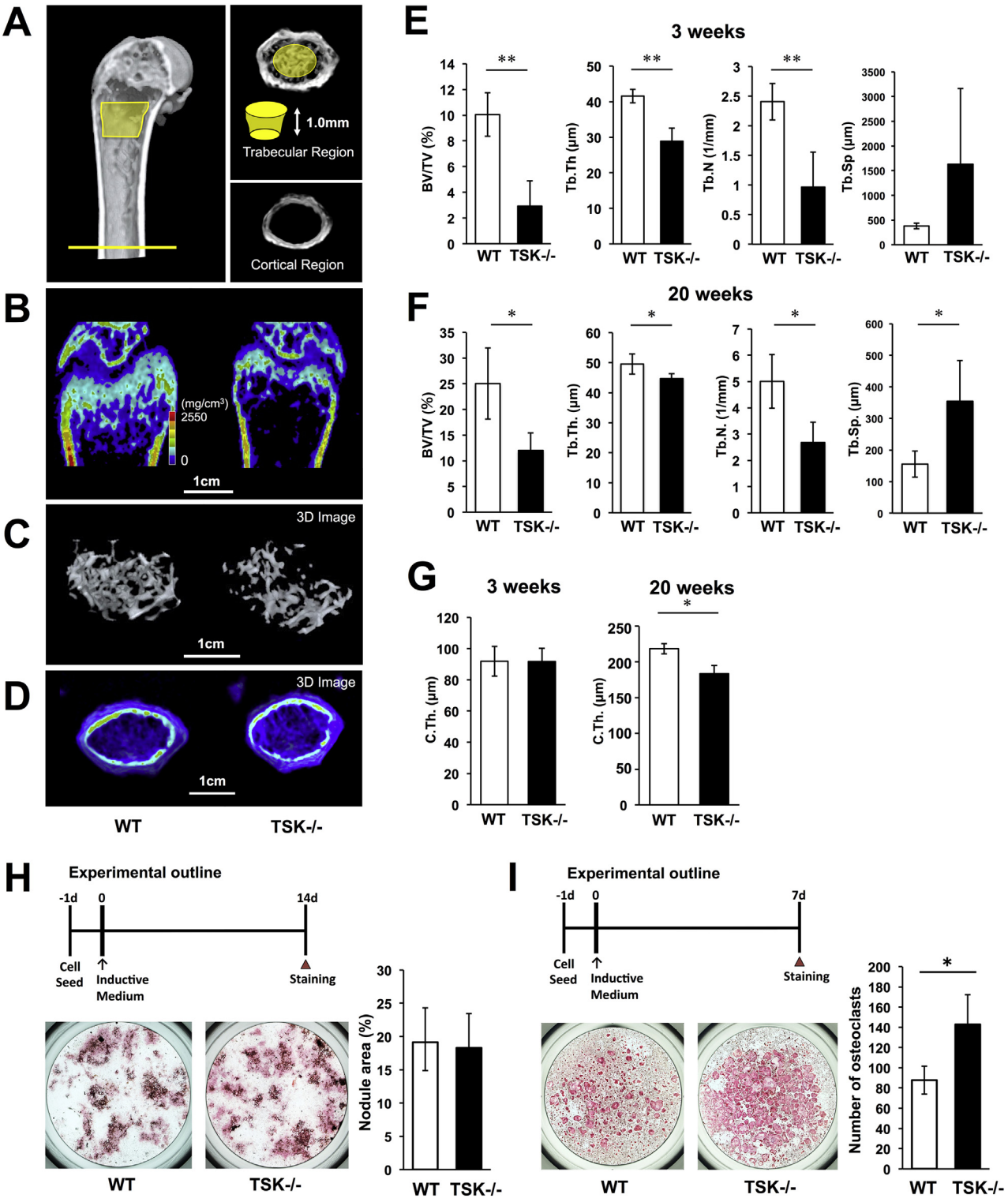

Fig. 2. Reduced femur bone mass in TSK−/− mice. (A) Femurs were analysed separately in the trabecular region (cylinder: 0.4 mm proximal to the distal growth plate, 1.0 mm in height) and in the cortical region (cylinder: middle of the femur, 1.0 mm in height). (B) μCT images of femurs of 3-week-old WT and TSK−/− mice. (C) Three dimensional (3D) images of trabecular bones of 3-week-old WT and TSK−/− mice. (D) 3D images of cortical bones of 3-week-old WT and TSK−/− mice. (E, F) Parameters for the trabecular region, including bone volume/tissue volume ratio (BV/TV), trabecular number (Tb.N.), trabecular thickness (Tb.Th.), and trabecular separation (Tb.Sp.) in 3 and 20-week-old WT and TSK−/− mice. Data are presented as mean ± SD with 4 mice in each genotype group ($^{*}p < 0.05$, $^{**}p < 0.01$ vs. WT littermates, $n = 4$). (G) Cortical thickness (C.Th.) of 3- and 20-week-old WT and TSK−/− mice. C.Th. was measured at 8 points. Data are reported as mean ± SD ($^{*}p < 0.05$ vs. WT littermates, $n = 4$). (H) Experimental outline of osteoblast differentiation. Bone marrow cells were harvested from femur of 20-week-old WT and TSK−/− mice and cultured with osteoinductive medium for 14 days and mineralized nodules were stained by alizarin red S. There was no significant difference in nodule formation activity between WT and TSK−/− osteoblasts. (I) Experimental outline of osteoclast differentiation. Bone marrow cells were harvested from femur of 20-week-old WT and TSK−/− mice and cultured with osteoclast-inductive medium for 7 days. And then, stained by tartrate-resistant acid phosphatase (TRAP) staining and the number of osteoclasts was counted. The number of TRAP-positive cells was significantly increased in TSK−/− mice.

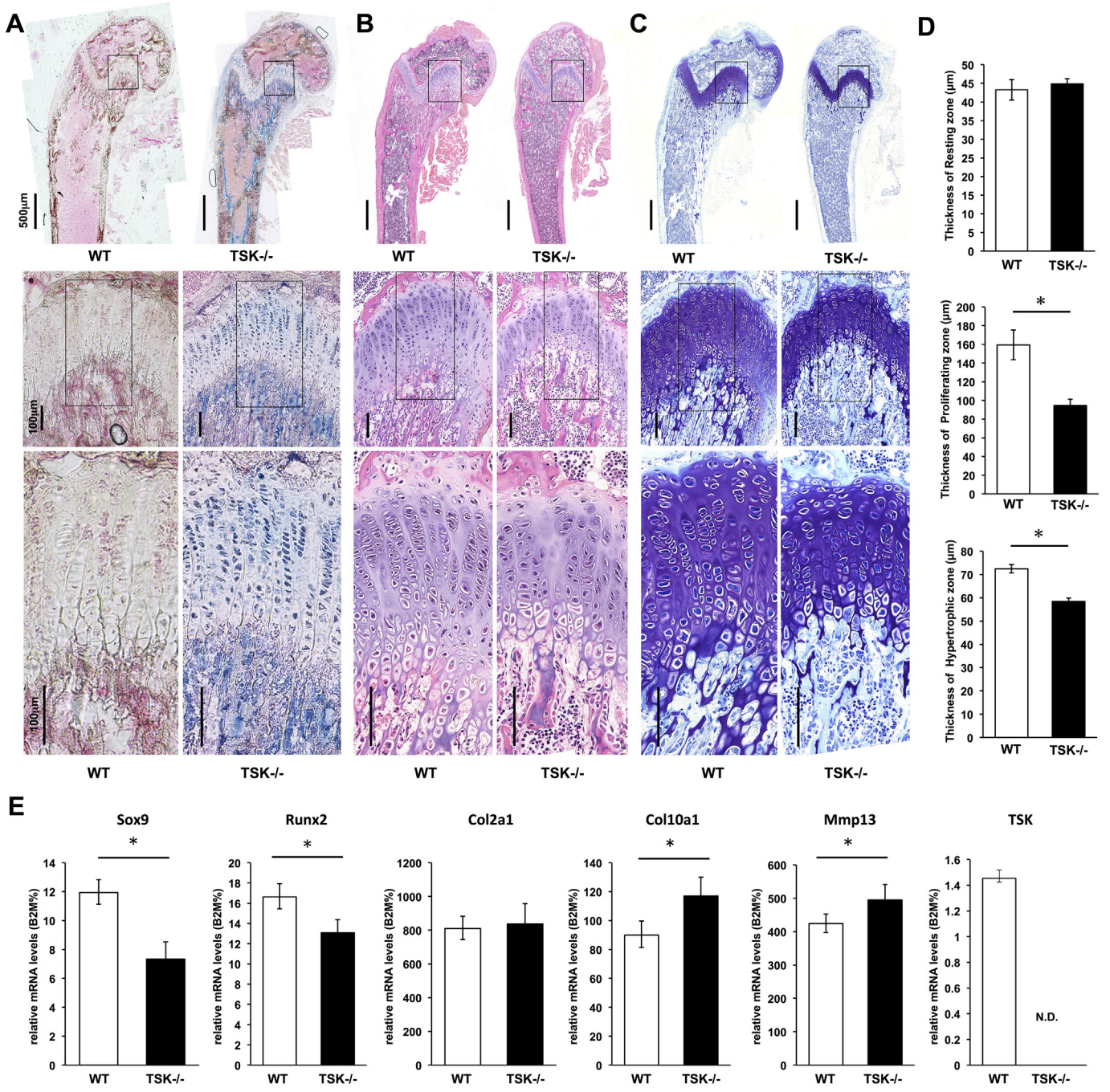

Fig. 3. Shortened and morphologically abnormal growth plate and abnormal expression of chondrogenic markers in the growth plate of TSK−/− mutant femurs. (A) Images of sagittal sections of 3-week-old TSK−/− mouse femurs stained with β-gal staining (blue) showing TSK expression patterns in the femur. Counter-staining was performed with nuclear fast red. Expression of TSK was observed in chondrocytes in the growth plate and in cells around the trabecular bone and cortical bone in the femurs of TSK−/− mice. No endogenous β-gal activity was observed in the femurs of WT mice. (B) Images of sagittal sections of 3-week-old WT and TSK−/− mouse femurs stained with haematoxylin and eosin. The columnar arrays of chondrocytes are disturbed in TSK−/− mice. (C) Images of sagittal sections of 3-week-old WT and TSK−/− mouse femurs stained with toluidine blue. Growth plate thickness was reduced in TSK−/− mice. (D) Quantitative analysis of growth plate thickness at the resting, proliferating, and hypertrophic zones in 3-week-old WT and TSK−/− mice. The thickness of each zone was measured at 10 points. Results are expressed as the mean from 3 mice in each group (*$p < 0.05$ vs. WT littermates, $n = 3$). (E) Chondrogenic marker mRNA levels in growth plate cells of WT and TSK−/− mice obtained by microdissection according to RT-PCR (*$p < 0.05$ vs. WT littermates, $n = 5$).

in TSK−/− mice at 3 weeks of age. This decrease was associated with a significant reduction in the relative size of the proliferating and hypertrophic zones of growth plates in TSK−/− mice (Fig. 3D), though the thickness of the resting zone was not reduced in TSK−/− mice (Fig. 3D). Thus, in TSK−/− mice, a reduction in the growth plate thickness and abnormal chondrocytes were observed, suggesting that the skeletal abnormalities observed in TSK−/− mice are due to a dysfunction of chondrocytes located in growth plate.

3.4. Abnormal expression of chondrogenic marker genes in femur growth plates of TSK−/− mice

To examine whether deficiency of TSK function affects endochondral ossification at the molecular level, expression levels of chondrogenesis marker genes were quantified by RT-PCR. Femur growth plates were individually captured and microdissected from cryosections. TSK deletion resulted in a significant decrease in *Sox9*

and *Runx2* expression and a significant increase in mid-to-late chondrogenesis marker genes such as *Col10a1* and *Mmp13* in growth plate chondrocytes (Fig. 3E). Expression of *Col2a1* was not significantly altered in TSK−/− mice (Fig. 3E).

3.5. TSK related to chondrogenic differentiation in ATDC5 cells

The ATDC5 cell line is a mouse embryonal carcinoma-derived chondrogenic cell line and an appropriate *in vitro* model for studying chondrogenesis [33–35]. To estimate the effects of *TSK* gene on chondrogenesis, an siRNA designed to target the *TSK* gene was transfected into ATDC5 cells. In order to evaluate the effect of decreased expression of *TSK* on differentiation, ATDC5 cells were seeded at an overconfluent cell density, and micromass culture was performed in the absence or presence of *TSK* siRNA for 7 days (Fig. 4A). Then, ATDC5 cell micromass culture was subjected to alcian blue staining, which specifically stains sulphated proteoglycans. Results revealed that decreased expression of *TSK* resulted in significantly increased production of glycosaminoglycans (Fig. 4C and D).

A decrease in *TSK* mRNA levels accompanied by an increase in chondrogenesis in ATDC5 cells would indicate that TSK may inhibit signaling molecules that accelerate chondrocyte differentiation. We therefore attempted to determine the effect of TSK loss on chondrocyte differentiation marker genes by transfecting siRNA into ATDC5 cells. A chondrogenic inductive medium was added 3 days after transfection of *TSK* siRNA into ATDC5 cells. After 3 and 7 days of incubation with chondrogenic inductive medium, total RNA was extracted and RT-PCR analysis was performed (Fig. 4B). We confirmed that *TSK* mRNA expression was suppressed in the

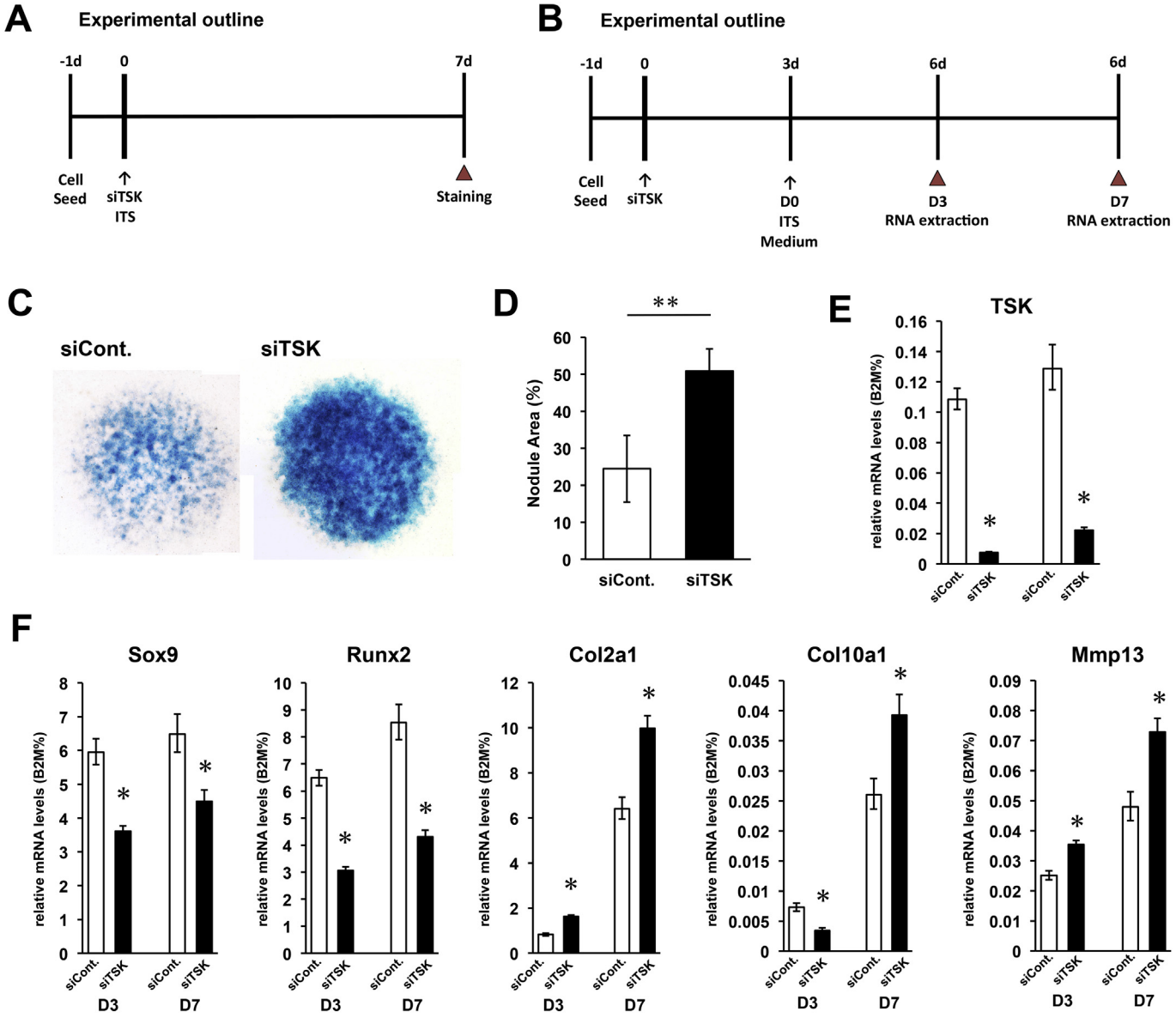

Fig. 4. Decreased TSK expression promotes proliferation and differentiation of ATDC5 cells. (A) Experimental outline of micromass culture. Micromass culture was performed in the absence or presence of *TSK* siRNA for 7 days and cells stained with alcian blue staining. (B) Experimental outline of gene assay. A chondrogenic inductive medium was added 3 days after transfection of *TSK* siRNA into ATDC5 cells. After 3 and 7 days of incubation with chondrogenic inductive medium, total RNA was extracted and RT-PCR analysis was performed. (C) ATDC5 cells in micromass cultures were stained with alcian blue on day 7. (D) Quantification of nodule areas in micromass culture (**$p < 0.01$ vs. control, $n = 6$). (E) Expression level of *TSK* mRNA was suppressed in siRNA-transfected cells with chondrogenic induction in each time point (Day 3, Day 7). (F) Relative mRNA expression levels of chondrogenic marker genes such as Sox9, Runx2, Col2a1, Col10a1, and MMP13 as measured by RT-PCR (*$p < 0.05$ vs. control, $n = 3$).

transfection group at each experimental time point (Fig. 4E). We also found that expression of several chondrogenic marker genes, *Sox9* and *Runx2* in cultures transfected with *TSK* siRNA were significantly lower than those in control cells under chondrogenic inductive conditions (Fig. 4F). Conversely, expression levels of *Col2a1*, *Col10a1*, and *Mmp13* were significantly and sequentially up-regulated following *TSK* siRNA transfection when cells were induced by chondrogenic medium (Fig. 4F). This indicates that the increased differentiation of ATDC5 cells under *TSK* knockdown is due to down-regulation of chondrogenic markers such as Sox9, Runx2 and up-regulation of mid-to-late chondrogenic markers such as *Col2a1*, *Col10a1*, and *Mmp13*. These results are consistent with those of the *in vivo* TSK knockout gene expression analysis.

4. Discussion

In previous studies, TSK was found to be a significant coordinator of multiple pathways through the regulation of extracellular signaling molecules such as BMP, Wnt, FGF, and TGF-β [5,15–17]. The purpose of our investigation was to expand our understanding of the function of TSK. In this study, we investigated the function of TSK during long bone growth comparing TSK−/− and WT mice.

TSK−/− mice exhibited novel phenotypic features such as a reduction in weight and a short stature due to decreased longitudinal bone growth coupled with decreased bone mass. As observed with biglycan knockout mice, these phenotypes were not lethal [11,12]. These phenotypic features were observed in both juvenile and adult TSK−/− mice. Whole-mount β-gal staining using TSK−/− mice at P0 exhibited TSK's expression pattern in humerus and costal cartilage (Data not shown). Reduction in growth plate thickness and abnormal chondrocyte shape was also observed, suggesting that the skeletal abnormalities of TSK−/− mice were due to dysfunction of chondrogenic differentiation at growth plate. Interestingly, there was no significant difference observed in the size of cranium in WT and TSK−/− mice. TSK doesn't affect the size of the cranium which develop via intramembranous ossification (data not shown).

In addition, TSK deletion resulted in significant down-regulation of chondrogenesis marker genes, Sox9 and Runx2, and up-regulation of mid-to-late chondrogenesis marker genes in growth-plate chondrocytes.

The micromass culture experiment using siRNA transfection of chondrogenic cell line, ATDC5 cells revealed that decreased *TSK* expression resulted in chondrogenesis acceleration. These results indicate that TSK may inhibit signaling molecules that accelerate chondrogenesis. Furthermore, mRNA expression levels of key chondrogenic markers were down-regulated and those of mid-to-late chondrogenic markers were up-regulated under *TSK* knockdown conditions.

Summarizing both the *in vivo* and *in vitro* data, TSK appears to control bone elongation and bone mass by modulating growth plate chondrocyte function and consequently, overall body size. Longitudinal bone growth is fundamentally determined by the rate of growth-plate chondrogenesis [35]. Disorders of growth plate function produce a wide range of phenotypes from severe skeletal dysplasia to short or tall stature [36]. This is the first report of TSK's significant functional role in skeletogenesis.

Decrease in bone mass is not only due to endochondral ossification and we considered contribution of TSK's defects in osteoblasts and osteoclasts. The result indicates that TSK also possibly effects bone volume by regulating osteoclast differentiation in bone marrow in adult stage. These data suggest that TSK plays multiple roles both in bone growth and bone metabolism. Further research should be continued to clarify broad functions of TSK in bone metabolism.

Sox9 and *Runx2* are key transcription factors that play essential roles in chondrogenesis. *Sox9* inhibits differentiation of chondrocyte to the late stages of endochondral ossification [37–40]. *Sox 9* is controlled by multiple signal pathways such as Wnt [41,42], BMP [43], TGF [44], FGF [45]. In chondrocyte differentiation, Wnt pathway suppresses the expression of Sox9. On the other hand, BMP, TGF, and FGF pathways upregulate the expression of *Sox9.* Simultaneously, BMP pathway upregulates the expression of *Col10a1* and *MMP13* in a different pathway of controlling *Sox9*. TSK has been reported as an important coordinator of numerous pathways by suppressing their functions. Under conditions of TSK's deficient or knockdown, we can assume that each pathway is enhanced, and as a result, expression of *Sox9* decreased and the expression level of *Col10a1* and *MMP13* increased.

Mid-to-late chondrocyte marker genes, as *Col10a1* and *MMP13*, are associated with the differentiation of hypertrophic chondrocytes to endochondral ossification [46]. The acceleration of differentiation of hypertrophic chondrocyte reduces the total number of chondrocytes and induces premature ossification, thus compromising skeletal development. We found that expression levels of *Col10a1* and *MMP13* in growth plate chondrocytes in TSK−/− mice femur were significantly elevated. Similarly, expression levels of *Col2a1*, *Col10a1,* and *MMP13* in a *TSK* knockdown cell line were significantly up-regulated over time. These data suggested that *TSK* deletion induced the differentiation of hypertrophic chondrocyte to immature ossification by elevation of *Col10a1* and *MMP13*.

Runx2 also has important function in the growth plate, as it promotes the differentiation of proliferative chondrocytes into hypertrophic chondrocytes [47]. *Runx2* is also controlled by multiple signal pathways such as Notch [48], BMP [49]. In chondrogenesis, Notch pathway suppresses the expression of Runx2, and the other pathways such as BMP pathways upregulate the expression of Runx2. We can assume that conditions of TSK's deficient or knockdown enhanced each pathway individually, and as a result, the expression level of *Runx2* decreased.

In summary, our results suggest that the absence of TSK causes a reduction in the number of proliferative chondrocytes and an acceleration of premature endochondral ossification due to accelerated hypertrophic chondrocyte differentiation. The results of *in vitro* and *in vivo* RT-PCR showing discrepancy of each gene expression suggest that TSK works as an important coordinator of numerous pathways and each pathway relates in complexity.

Activity of growth plate chondrocytes is controlled not only by paracrine factors, such as FGFs, BMPs, and Wnts, but also by multiple hormones, such as GH and IGF-1. Nutritional intake greatly affects endocrine regulators such as IGF-1, leptin, thyroid hormone, sex steroids, and glucocorticoids [50]; however, in this study, there was no significant difference in food intake between WT littermates and TSK−/− mice.

SLRPs have diverse functions that involve interacting with various cell surface receptors, growth factors, cytokines, and other ECM components, modulating cellular functions [51]. Previous studies have clarified the important roles of SLRPs on bone physiology and disease. TSK is structurally categorized as a member of the class IV SLRPs [6], but it exhibits functional properties of class I SLRPs as it works as a BMP inhibitor that forms a ternary complex with BMP and chordin [5,10]. SLRP depletion causes degenerative diseases or phenotypes, including osteoporosis, ectopic bone formation [8], and short stature [9]. The phenotypic features of TSK−/− mice exhibited in this study are similar to those of biglycan-deficient mice [11,12]. Biglycan and decorin modulate skeletal growth and bone formation through interacting with TGF-β. The absence of biglycan and decorin leads to TGF-β-hyperactive cells, which exhibit accelerated proliferation and undergo apoptosis

prematurely [46]. Asporin, another class I SLRP, also interacts with TGF-β and attenuates its signal effect by inhibiting it from binding to its receptor. TGF-β1 is involved in cell proliferation, differentiation, and apoptosis and plays an important role in the development and homeostasis of a wide range of tissues [14]. TGF-β1 is a key regulator of chondrocyte proliferation and differentiation as well as collagen proliferation [52]. However, since the uncontrolled action of TGF-β1 may cause several problems, such as abnormal cartilage growth and ossification, it is under the control of various regulatory mechanisms [14]. Previous studies involving TSK−/− mice have concluded that TSK binds directly to TGF-β1 and modulates TGF-β1 signaling [17]. These studies indicated that TSK may maintain cells that are TGF-β1-dependent, such as chondrocytes. Namely, TSK may modulate chondrogenesis by suppressing TGF-β. Excessive TGF-β signaling is associated with congenital connective tissue diseases, and some of these are characterized by short stature and short bones [53]. Relationship between Tsukushi and any human diseases have not been clarified yet. Since TSK's multiple function on several paracrine factors, there are possibilities that TSK have relationships with human skeletal diseases such as Weill–Marchesani syndrome, Geleophysic dysplasia, Acromicric dysplasia which is associate with TGF-β activity. We suggest that by elucidating the function of TSK, new therapeutic methods for skeletal systemic diseases may be discovered.

For the regenerative therapy, quality control of cell products is necessary to conduct the treatment effectively. We have expected that the expression of TSK is one of the candidates for indicators of quality control check in chondrogenic cells.

Based on the present study, we conclude that TSK regulates skeletal development by modulating chondrocyte activity. TSK is widely expressed in the bone area not only in growth plate chondrocytes but also in cells around the trabecular bone and cortical bone. Significantly thinner cortical bones in the femurs of adult TSK−/− mice suggest that TSK may have other roles in modulating bone and cartilage metabolic homeostasis. TSK is a newly identified factor among SLRPs and some of its functions have now been revealed.

5. Conclusion

TSK is a newly identified factor among SLRPs and controls bone growth, including bone elongation and bone mass, by modulating growth plate chondrocyte function and consequently, overall body size.

Acknowledgments

The authors thank Takanori Iwata of the Institute of Advanced Biomedical Engineering and Science, Tokyo Women's Medical University, for excellent expert advice; Terumasa Umemoto of the International Research Center for Medical Science, Kumamoto University, for valuable advice and suggestions; Mami Kokubo of the Institute of Advanced Biomedical Engineering and Science, Tokyo Women's Medical University, for technical support; Masaki Noda of 1. Tokyo Medical and Dental University, 2. Yokohama City Minato Red Cross Hospital, for practical advice; Yoichi Ezura of Tokyo Medical and Dental University, for technical support and advice; Kazuhiro Aoki of Tokyo Medical and Dental University, for advice and suggestions; This study was partially supported by the Creation of Innovation Centers for Advanced Interdisciplinary Research Areas Program in the Project for Developing Innovation Systems “Cell Sheet Tissue Engineering Center (CSTEC)” from the Ministry of Education, Culture, Sports, Science and Technology (MEXT), Japan.

References

[1] Kronenberg HM. Developmental regulation of the growth plate. Nature 2003;423:332–6. http://dx.doi.org/10.1038/nature01657.
[2] Kobayashi T, Kronenberg HM. Overview of skeletal development. In: Hilton MJ, editor. Skeletal development and repair: methods and protocols. Totowa, NJ: Humana Press; 2014. p. 3–12. http://dx.doi.org/10.1007/978-1-62703-989-5_1.
[3] Long F, Ornitz DM. Development of the endochondral skeleton. Cold Spring Harb Perspect Biol 2013;5:1–20. http://dx.doi.org/10.1101/cshperspect.a008334.
[4] Kozhemyakina E, Lassar AB, Zelzer E. A pathway to bone: signaling molecules and transcription factors involved in chondrocyte development and maturation. Development 2015;142:817–31. http://dx.doi.org/10.1242/dev.105536.
[5] Ohta K, Lupo G, Kuriyama S, Keynes R, Holt CE, Harris WA, et al. Tsukushi functions as an organizer inducer by inhibition of BMP activity in cooperation with chordin. Dev Cell 2004;7:347–58. http://dx.doi.org/10.1016/j.devcel.2004.08.014.
[6] Iozzo RV, Schaefer L. Proteoglycan form and function: a comprehensive nomenclature of proteoglycans. Matrix Biol 2015;42:11–55. http://dx.doi.org/10.1016/j.matbio.2015.02.003.
[7] Merline R, Schaefer RM, Schaefer L. The matricellular functions of small leucine-rich proteoglycans (SLRPs). J Cell Commun Signal 2009;3:323–35. http://dx.doi.org/10.1007/s12079-009-0066-2.
[8] Nikitovic D, Aggelidakis J, Young MF, Iozzo RV, Karamanos NK, Tzanakakis GN. The biology of small leucine-rich proteoglycans in bone pathophysiology. J Biol Chem 2012;287:33926–33. http://dx.doi.org/10.1074/jbc.R112.379602.
[9] Geerkens C, Vetter U, Just W, Fedarko NS, Fisher LW, Young MF, et al. The X-chromosomal human biglycan gene BGN is subject to X inactivation but is transcribed like an X-Y homologous gene. Hum Genet 1995;96:44–52. http://dx.doi.org/10.1007/BF00214185.
[10] Ohta K, Kuriyama S, Okafuji T, Gejima R, Ohnuma S, Tanaka H. Tsukushi cooperates with VG1 to induce primitive streak and Hensen's node formation in the chick embryo. Development 2006;133:3777–86. http://dx.doi.org/10.1242/dev.02579.
[11] Xu T, Bianco P, Fisher LW, Longenecker G, Smith E, Goldstein S, et al. Targeted disruption of the biglycan gene leads to an osteoporosis-like phenotype in mice. Nat Genet 1998;20:78–82. http://dx.doi.org/10.1038/1746.
[12] Corsi a, Xu T, Chen XD, Boyde A, Liang J, Mankani M, et al. Phenotypic effects of biglycan deficiency are linked to collagen fibril abnormalities, are synergized by decorin deficiency, and mimic Ehlers-Danlos-like changes in bone and other connective tissues. J Bone Min Res 2002;17:1180–9. http://dx.doi.org/10.1359/jbmr.2002.17.7.1180.
[13] Young MF, Bi Y, Ameye L, Chen XD. Biglycan knockout mice: new models for musculoskeletal diseases. Glycoconj J 2003;19:257–62. http://dx.doi.org/10.1023/A:1025336114352.
[14] Kizawa H, Kou I, Iida A, Sudo A, Miyamoto Y, Fukuda A, et al. An aspartic acid repeat polymorphism in asporin inhibits chondrogenesis and increases susceptibility to osteoarthritis. Nat Genet 2005;37:138–44. http://dx.doi.org/10.1038/ng1496.
[15] Ohta K, Ito A, Kuriyama S, Lupo G, Kosaka M, Ohnuma S-I, et al. Tsukushi functions as a Wnt signaling inhibitor by competing with Wnt2b for binding to transmembrane protein Frizzled4. Proc Natl Acad Sci U S A 2011;108:14962–7. http://dx.doi.org/10.1073/pnas.1100513108.
[16] Morris SA, Almeida AD, Tanaka H, Ohta K, Ohnuma SI. Tsukushi modulates Xnr2, FGF and BMP signaling: regulation of Xenopus germ layer formation. PLoS One 2007;2. http://dx.doi.org/10.1371/journal.pone.0001004.
[17] Niimori D, Kawano R, Felemban A, Niimori-Kita K, Tanaka H, Ihn H, et al. Tsukushi controls the hair cycle by regulating TGF-β1 signaling. Dev Biol 2012;372:81–7. http://dx.doi.org/10.1016/j.ydbio.2012.08.030.
[18] Dellett M, Hu W, Papadaki V, Ohnuma S. Small leucine rich proteoglycan family regulates multiple signalling pathways in neural development and maintenance. Dev Growth Differ 2012;54:327–40. http://dx.doi.org/10.1111/j.1440-169X.2012.01339.x.
[19] Ito A, Shinmyo Y, Abe T, Oshima N, Tanaka H, Ohta K. Tsukushi is required for anterior commissure formation in mouse brain. Biochem Biophys Res Commun 2010;402:813–8. http://dx.doi.org/10.1016/j.bbrc.2010.10.127.
[20] Hung IH, Yu K, Lavine KJ, Ornitz DM. FGF9 regulates early hypertrophic chondrocyte differentiation and skeletal vascularization in the developing stylopod. Dev Biol 2007;307:300–13. http://dx.doi.org/10.1016/j.ydbio.2007.04.048.
[21] Lazarus JE, Hegde A, Andrade AC, Nilsson O, Baron J. Fibroblast growth factor expression in the postnatal growth plate. Bone 2007;40:577–86. http://dx.doi.org/10.1016/j.bone.2006.10.013.
[22] Liu Z, Lavine KJ, Hung IH, Ornitz DM. FGF18 is required for early chondrocyte proliferation, hypertrophy and vascular invasion of the growth plate. Dev Biol 2007;302:80–91. http://dx.doi.org/10.1016/j.ydbio.2006.08.071.
[23] Mancilla EE, De Luca F, Uyeda JA, Czerwiec FS, Baron J. Effects of fibroblast growth factor-2 on longitudinal bone growth. Endocrinology 1998;139:2900–4. http://dx.doi.org/10.1210/en.139.6.2900.
[24] De Luca F, Barnes KM, Uyeda JA, De-Levi S, Abad V, Palese T, et al. Regulation of growth plate chondrogenesis by bone morphogenetic protein-2. Endocrinology 2001;142:430–6. http://dx.doi.org/10.1210/endo.142.1.7901.

[25] Nilsson O, Parker EA, Hegde A, Chau M, Barnes KM, Baron J. Gradients in bone morphogenetic protein-related gene expression across the growth plate. J Endocrinol 2007;193:75–84. http://dx.doi.org/10.1677/joe.1.07099.
[26] Pogue R, Lyons K. BMP signaling in the cartilage growth plate. Curr Top Dev Biol 2006;76:1–48. http://dx.doi.org/10.1016/S0070-2153(06)76001-X.
[27] Andrade AC, Nilsson O, Barnes KM, Baron J. Wnt gene expression in the postnatal growth plate: regulation with chondrocyte differentiation. Bone 2007;40:1361–9. http://dx.doi.org/10.1016/j.bone.2007.01.005.
[28] Kuss P, Kraft K, Stumm J, Ibrahim D, Vallecillo-Garcia P, Mundlos S, et al. Regulation of cell polarity in the cartilage growth plate and perichondrium of metacarpal elements by HOXD13 and WNT5A. Dev Biol 2014;385:83–93. http://dx.doi.org/10.1016/j.ydbio.2013.10.013.
[29] Haque SF, Izumi S-I, Aikawa H, Suzuki T, Matsubayashi H, Murano T, et al. Anesthesia and acoustic stress-induced intra-uterine growth retardation in mice. J Reprod Dev 2004;50:185–90. http://dx.doi.org/10.1262/jrd.50.185.
[30] Hoogendam J, Parlevliet E, Miclea R, Löwik CWGM, Wit JM, Karperien M. Novel early target genes of parathyroid hormone-related peptide in chondrocytes. Endocrinology 2006;147:3141–52. http://dx.doi.org/10.1210/en.2006-0075.
[31] Kawamoto T. Use of a new adhesive film for the preparation of multi-purpose fresh-frozen sections from hard tissues, whole-animals, insects and plants. Arch Histol Cytol 2003;66:123–43. http://dx.doi.org/10.1679/aohc.66.123.
[32] Matsuzaki Y, Umemoto T, Tanaka Y, Okano T, Yamato M. β2-Microglobulin is an appropriate reference gene for RT-PCR-based gene expression analysis of hematopoietic stem cells. Regen Ther 2015;1:91–7. http://dx.doi.org/10.1016/j.reth.2015.04.003.
[33] Altaf FM, Hering TM, Kazmi NH, Yoo JU, Johnstone B. Ascorbate-enhanced chondrogenesis of ATDC5 cells. Eur Cells Mater 2006;12:64–9.
[34] Shukunami C, Shigeno C, Atsumi T, Ishizeki K, Suzuki F, Hiraki Y. Chondrogenic differentiation of clonal mouse embryonic cell line ATDC5 in vitro: differentiation-dependent gene expression of parathyroid hormone (PTH)/PTH-related peptide receptor 1996;133:457–68. http://dx.doi.org/10.1083/jcb.133.2.457.
[35] Yao Y, Wang Y. ATDC5: an excellent in vitro model cell line for skeletal development. J Cell Biochem 2013;114:1223–9. http://dx.doi.org/10.1002/jcb.24467.
[36] Baron J, Sävendahl L, De Luca F, Dauber A, Phillip M, Wit JM, et al. Short and tall stature: a new paradigm emerges. Nat Rev Endocrinol 2015;11:735–46. http://dx.doi.org/10.1038/nrendo.2015.165.
[37] Dudek SM, Chiang ET, Camp SM, Guo Y, Zhao J, Brown ME, et al. Abl tyrosine kinase phosphorylates nonmuscle Myosin light chain kinase to regulate endothelial barrier function. Mol Biol Cell 2010;21:4042–56. http://dx.doi.org/10.1091/mbc.E09.
[38] Hattori T, Müller C, Gebhard S, Bauer E, Pausch F, Schlund B, et al. SOX9 is a major negative regulator of cartilage vascularization, bone marrow formation and endochondral ossification. Development 2010;137:901–11. http://dx.doi.org/10.1242/dev.045203.
[39] Ikeda T, Kamekura S, Mabuchi A, Kou I, Seki S, Takato T, et al. The combination of SOX5, SOX6, and SOX9 (the SOX trio) provides signals sufficient for induction of permanent cartilage. Arthritis Rheum 2004;50:3561–73. http://dx.doi.org/10.1002/art.20611.
[40] Saito T, Ikeda T, Nakamura K, Chung U, Kawaguchi H. S100A1 and S100B, transcriptional targets of SOX trio, inhibit terminal differentiation of chondrocytes. EMBO Rep 2007;8:504–9. http://dx.doi.org/10.1038/sj.embor.7400934.
[41] Day TF, Guo X, Garrett-Beal L, Yang Y. Wnt/β-catenin signaling in mesenchymal progenitors controls osteoblast and chondrocyte differentiation during vertebrate skeletogenesis. Dev Cell 2005;8:739–50. http://dx.doi.org/10.1016/j.devcel.2005.03.016.
[42] Hill TP, Später D, Taketo MM, Birchmeier W, Hartmann C. Canonical Wnt/β-catenin signaling prevents osteoblasts from differentiating into chondrocytes. Dev Cell 2005;8:727–38. http://dx.doi.org/10.1016/j.devcel.2005.02.013.
[43] Yoon BS, Ovchinnikov DA, Yoshii I, Mishina Y, Behringer RR, Lyons KM. Bmpr1a and Bmpr1b have overlapping functions and are essential for chondrogenesis in vivo. Proc Natl Acad Sci U S A 2005;102:5062–7. http://dx.doi.org/10.1073/pnas.0500031102.
[44] Blitz E, Sharir A, Akiyama H, Zelzer E. Tendon-bone attachment unit is formed modularly by a distinct pool of Scx- and Sox9-positive progenitors. Development 2013;140:2680–90. http://dx.doi.org/10.1242/dev.093906.
[45] Murakami S, Kan M, McKeehan WL, de Crombrugghe B. Up-regulation of the chondrogenic Sox9 gene by fibroblast growth factors is mediated by the mitogen-activated protein kinase pathway. Proc Natl Acad Sci U S A 2000;97:1113–8. http://dx.doi.org/10.1073/PNAS.97.3.1113.
[46] Mirzamohammadi F, Papaioannou G, Inloes JB, Rankin EB, Xie H, Schipani E, et al. Polycomb repressive complex 2 regulates skeletal growth by suppressing Wnt and TGF-β signalling. Nat Commun 2016;7:12047. http://dx.doi.org/10.1038/ncomms12047.
[47] Kozhemyakina E, Lassar AB, Zelzer E. A pathway to bone: signaling molecules and transcription factors involved in chondrocyte development and maturation. Development 2015;142:817–31. http://dx.doi.org/10.1242/dev.105536.
[48] Zamurovic N, Cappellen D, Rohner D, Susa M. Coordinated activation of Notch, Wnt, and transforming growth factor-β signaling pathways in bone morphogenic protein 2-induced osteogenesis: notch target gene Hey1 inhibits mineralization and Runx2 transcriptional activity. J Biol Chem 2004;279:37704–15. http://dx.doi.org/10.1074/jbc.M403813200.
[49] Lee K, Hong S, Bae S. Both the Smad and p38 MAPK pathways play a crucial role in Runx2 expression following induction by transforming growth factor-b and bone morphogenetic protein. Oncogene 2002:7156–63. http://dx.doi.org/10.1038/sj.onc.1205937.
[50] Bi Y, Stuelten CH, Kilts T, Wadhwa S, Iozzo RV, Robey PG, et al. Extracellular matrix proteoglycans control the fate of bone marrow stromal cells. J Biol Chem 2005;280:30481–9. http://dx.doi.org/10.1074/jbc.M500573200.
[51] Merline R, Schaefer RM, Schaefer L. The matricellular functions of small leucine-rich proteoglycans (SLRPs). J Cell Commun Signal 2009;3:323–35. http://dx.doi.org/10.1007/s12079-009-0066-2.
[52] Grimaud E, Heymann D, Redini F. Recent advances in TGF-beta effects on chondrocyte metabolism. Potential therapeutic roles of TGF-beta in cartilage disorders. Cytokine Growth Factor Rev 2002;13:241–57.
[53] Hayata T, Ezura Y, Asashima M, Nishinakamura R, Noda M. Dullard/Ctdnep1 regulates endochondral ossification via suppression of TGF-β signaling. J Bone Min Res 2015;30:318–29. http://dx.doi.org/10.1002/jbmr.2343.